JOURNAL OF COMPUTATIONAL PHYSICS 120, 248–252 (1995)

A Finite Difference Scheme for the $K(2, 2)$ Compacton Equation

J. DE FRUTOS, M. A. LÓPEZ-MARCOS, AND J. M. SANZ-SERNA*

Departamento de Matemática Aplicada y Computación, Universidad de Valladolid, Valladolid, Spain

Received February 22, 1994; revised February 13, 1995

The $K(2, 2)$ equation, introduced by Rosenau and Hyman, is a wave equation that possesses solutions (compactons) that vanish outside a bounded interval of the spatial axis. A finite difference scheme for this equation is suggested that can successfully cope with compacton interactions leading to negative waves. We show rigorously that in those interactions a loss of smoothness of the solution necessarily takes place.

1. INTRODUCTION

The purpose of this paper is to present a finite difference method for the numerical integration of the $K(2, 2)$ equation introduced by Rosenau and Hyman [4]

$$u_T + (u^2)_X + (u^2)_{XXX} = 0. \tag{1}$$

The most salient feature of (1) is the existence of travelling wave solutions that are compactly supported, i.e., solutions that vanish outside a bounded X-interval. These solutions are called *compactons*. Thus, while the standard solitons of the Korteweg–de Vries or cubic Schroedinger equations become exponentially small as $|X| \to \infty$, compactons become actually 0 at a finite distance from the origin.

The analytic expression of the compactons is

$$u(X, T) = \frac{4\lambda}{3}\cos^2\frac{X - \lambda T - X_0}{4}, \quad |X - \lambda T - X_0| \le 2\pi,$$

with $u \equiv 0$ for $|X - \lambda T - X_0| > 2\pi$. Therefore compactons are continuous and possess continuous derivatives, but their second derivatives jump at $|X - \lambda T - X_0| = 2\pi$. The compacton solutions form a two-parameter family: λ represents the velocity and X_0 determines the initial location along the X-axis. Note that the compacton amplitude $4\lambda/3$ depends linearly on the velocity, but the compacton width 4π is independent of λ. When λ is negative the compacton takes negative values and moves to the left; it is then referred to as "anticompacton."

The numerical integration of (1) is not an easy task. Two sources of trouble are mentioned in [4]. First, the lack of smoothness of the compactons implies that high rates of convergence cannot be attained even when using methods that are formally of high order. Also the nonlinear "dispersive" term $(u^2)_{XXX}$, when expanded, includes a diffusionlike term $6u_Xu_{XX}$ that, in regions with $u_X > 0$, operates as a backward diffusion operator. Quoting from [4], "the solution would be unstable if it were not for the stabilizing nonlinear dispersion; this balance is easily lost in the numerical approximation."

There is a third source of difficulties not mentioned in [4]. As we rigorously prove in the appendix, smooth (H^2) solutions of (1) that are positive at $T = 0$ remain positive. Therefore solutions that start being positive and do not stay positive must leave the space H^2, no matter their initial smoothness. In this sense, the $K(2, 2)$ equation is similar to nonlinear hyperbolic conservation laws, like $u_T + (u^2)_X = 0$, in that smooth initial data give rise to nonsmooth solutions. In fact, our numerical experiments, clearly indicate that solutions of (1) are likely to develop *shocks*.

The numerical results presented in [4] were derived by means of pseudospectral techniques. We have experimented at length with spectral and pseudospectral methods and found that their performance is not very satisfactory. The sources of numerical difficulties discussed above imply that spectral and pseudospectral methods cannot operate unless supplemented by suitable filters. The behaviour of the filters we tried was erratic to say the least. Furthermore, it was not easy for us to tell apart the effects spuriously introduced by the filters from small features of the true solution being investigated.

For these reasons, we decided to try finite difference methods. The scheme presented in this paper is the only one, among those we have tried, that performs satisfactorily. The new scheme is presented in Section 2 and tested in Section 3.

2. THE SCHEME

In the numerical experiments, it is sometimes convenient to use a moving frame of reference $x = X - c_0T$, $t = T$, and write Eq. (1) as

$$u_t - c_0u_x + (u^2)_x + (u^2)_{xxx} = 0. \tag{2}$$

In the moving coordinates, compactons of parameter λ travel

* E-mail: frutos@cpd.uva.es, lopezmar@cpd.uva.es and sanzserna@cpd.uva.es.

0021-9991/95 $12.00

at a speed $\lambda - c_0$ and a judicious choice of c_0 may enable us to see a chosen compacton as stationary or almost stationary.

We add artificial viscosity in order to cater to solutions with shocks. It is well known that the viscosity terms can be added either directly to the difference scheme or to the differential equation itself. Here we chose the second alternative and introduce the regularized version of (2) given by

$$u_t - c_0 u_x + (u^2)_x + (u^2)_{xxx} + \varepsilon u_{xxxx} = 0, \quad \varepsilon > 0. \tag{3}$$

If $\{x_i\}$ represents a uniform grid with spacing h and $U_i(t)$ denotes the numerical approximation to $u(x_i, t)$, the difference method for (3) reads

$$\begin{aligned} &\frac{1}{120}\dot{U}_{j-2} + \frac{26}{120}\dot{U}_{j-1} + \frac{66}{120}\dot{U}_j + \frac{26}{120}\dot{U}_{j-1}\frac{1}{120}\dot{U}_{j+2} \\ &\quad - c_0\left(-\frac{1}{24h}U_{j-2} - \frac{10}{24h}U_{j-1} + \frac{10}{24h}U_{j+1} + \frac{1}{24h}U_{j+2}\right) \\ &\quad - \frac{1}{24h}U_{j-2}^2 - \frac{10}{24h}U_{j-1}^2 + \frac{10}{24h}U_{j+2}^2 + \frac{1}{24h}U_{j+2}^2 \\ &\quad - \frac{1}{2h^3}U_{j-2}^2 + \frac{2}{2h^3}U_{j-1}^2 - \frac{2}{2h^3}U_{j+1}^2 + \frac{1}{2h^3}U_{j+2}^2 \\ &\quad + \varepsilon\left(\frac{1}{h^4}U_{j-2} - \frac{4}{h^4}U_{j-1} + \frac{6}{h^4}U_j - \frac{4}{h^4}U_{j+1} + \frac{1}{h^4}U_{j+2}\right) = 0. \end{aligned} \tag{4}$$

The coefficients of the finite difference replacements of the operators ∂_x and ∂_x^3 and the coefficients of the time-derivatives $\dot{U}_j$ were used in [5] for the Korteweg–de Vries equation (see also [1]). These coefficients are chosen so that, when $\varepsilon = 0$, (4) is consistent of order 4. (Recall that this does not ensure that convergence of order $O(h^4)$ takes place; we are dealing with nonsmooth solutions.) The weights of the discretization of ∂_x^4 are standard; for $\varepsilon > 0$ the formal order of consistency is only 2.

3. NUMERICAL EXPERIMENTS

In the numerical experiments we work in an interval $0 \le x \le L$ with periodic boundary conditions. We set $h = L/J$, with J a positive integer and consider the grid points $x_j = jh$, $j = 1, \ldots, J$. Then (4) is a J-dimensional system of ordinary differential equations that we integrate by means of the standard implicit midpoint rule with a constant step size k. Recall that for $\dot{y} = f(y)$ the implicit midpoint rule is given by

$$\frac{y^{n+1} - y^n}{k} = f\left(\frac{y^{n+1} + y^n}{2}\right).$$

This method is consistent for second order, which matches that of the spatial discretization when $\varepsilon > 0$. It is also known that the midpoint rule is a suitable method for wave problems, where it may outperform higher order methods; see [2, 3].

TABLE I

One Compacton Solution

J	k	Amplitude error	Phase error
400	1/20	2.10E-5	4.31E-4
800	1/40	4.97E-6	1.21E-4
1600	1/80	1.29E-6	3.47E-5
3200	1/160	3.26E-7	8.55E-6
6400	1/320	8.14E-8	2.14E-6

Note. Errors at $t = 75$ for different discretization parameters, no artificial viscosity.

We have integrated the inviscid ($\varepsilon = 0$) equation with $c_0 = 2$, $L = 90$, $0 \le t \le 75$, and an initial condition corresponding to a compacton of parameter $\lambda = 1$. The compacton has amplitude $\frac{4}{3}$ and travels 75 units (in the moving frame of reference its speed is $1 - 2 = -1$). Table I provides, for various values of h and k, the errors in the amplitude and location of the numerically computed compacton at the final time $t = 75$. The amplitude of the numerical wave is *larger* than the true amplitude and correspondingly the numerical wave travels *more* than 75 units. The table shows that the errors are divided by 4 when h and k are simultaneously halved. The grid sizes reported are rather fine; for instance, $J = 400$ implies that there are about 56 grid points x_j within the compacton. Nevertheless, it is remarkable that the scheme yields such accurate results in a long time simulation of a nonsmooth solution of a potentially unstable equation. In actual fact, other finite difference or spectra discretizations are utterly unable to integrate the problem in the absence of artificial viscosity/filtering.

Experiments were also performed to assess the effect of the viscosity term. We integrated the compacton considered in Table I, but now we set $\varepsilon = 10^{-3}$ or $\varepsilon = 10^{-4}$. The values of h and k were chosen so small that the effect of numerical integration is negligible with respect to the perturbation introduced by the viscosity term. The results displayed in Table II nicely reveal an $O(\varepsilon)$ behaviour. Now the amplitude of the numerical solution is, as expected, less than $\frac{4}{3}$ and, correspondingly, the numerical wave travels less than 75 units. From

TABLE II

One Compacton Solution

ε	Amplitude error	Phase error
1E-3	2.53E-3	6.32E-2
1E-4	2.53E-4	6.32E-3

Note. Errors at $t = 75$ on a fine grid for different values of the viscosity parameter ε.

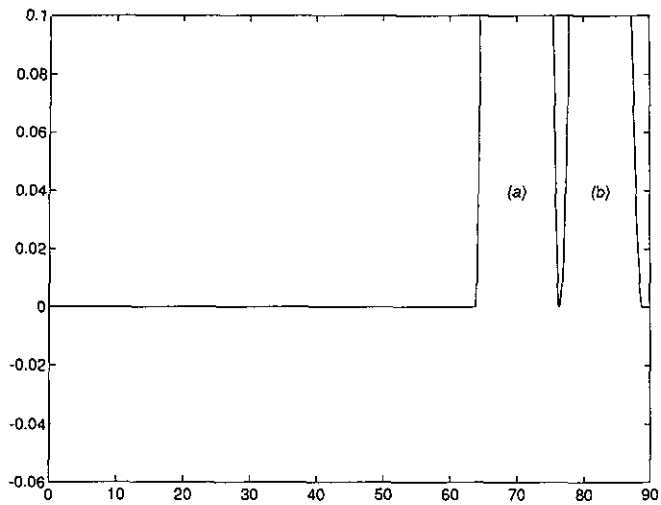

FIG. 1. *Compacton interaction, $t = 0$.*

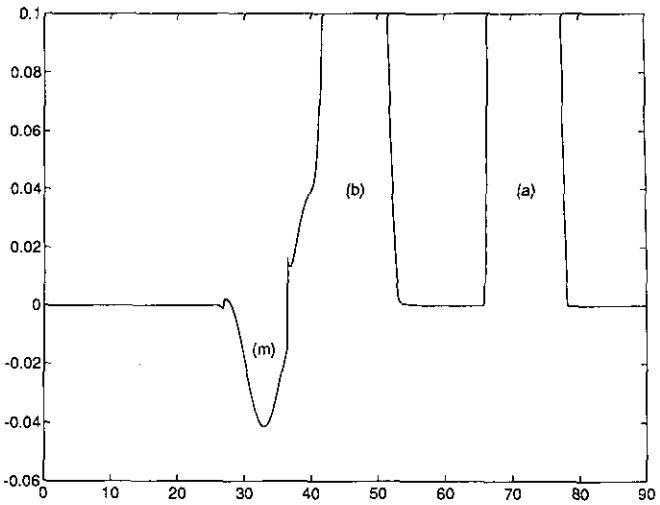

FIG. 3. Compacton interaction, $t = 20$.

these experiments we conclude that the introduction of the regularization term with $\varepsilon = 10^{-3}$ or $\varepsilon = 10^{-4}$ does not have a significant effect on the compacton motion; with $\varepsilon = 10^{-4}$ the amplitude damping in a long time integration is only of the order of 0.01%.

We finally describe an experiment involving the interaction of two compactons. The parameter values are $L = 90$, $c_0 = 2$, $\varepsilon = 10^{-4}$ and the solution is integrated in a time interval $0 \leq t \leq 75$. The initial condition (see Fig. 1) consists of two compactons that we call (a) and (b), with parameters $\lambda_a = 2$ and $\lambda_b = 0.5$ located next to each other. The taller compacton (a) is initially located at $x = 70$ and the shorter compacton (b) is initially located at $x = 70 + 4\pi$. Due to the value of c_0, compacton (a) is stationary while compacton (b) moves to the left with speed 1.5. The discretization parameters are $J = 6400$ ($h \simeq 0.014$) and $k = \frac{1}{320} \simeq 0.003$. For $J = 3200$, $k = \frac{1}{160}$ the integration could not be carried out until the final time $t = 75$.

Figure 2 corresponds to $t = 10$. Both compactons have provisionally merged into a single wave of height 2.662; a *negative* wave, labelled (m), has been born. The result in the appendix implies that the solution has left the space H^2 and in fact we see in the figure that a shock discontinuity has appeared between the waves (a) + (b) and (m). The overshoots in this and the following figures do not appear to be numerical artifacts; we have checked that they persist after grid refinement.

The situation at $t = 20$ is pictured in Fig. 3. Compactons (a) and (b) have emerged from the interaction and move with the expected velocities 0 and -1.5. The amplitudes of (a), (b), and (m) may be seen in Table III.

At $t = 30$ (Fig. 4), a new positive wave (c) has emerged from (b) and at $t = 40$ (Fig. 5) (m) is about to collide with (a). Figure 6, at $t = 45$, shows (m), emerging from the interaction and (c) colliding with (a). At this time the height of (a) is

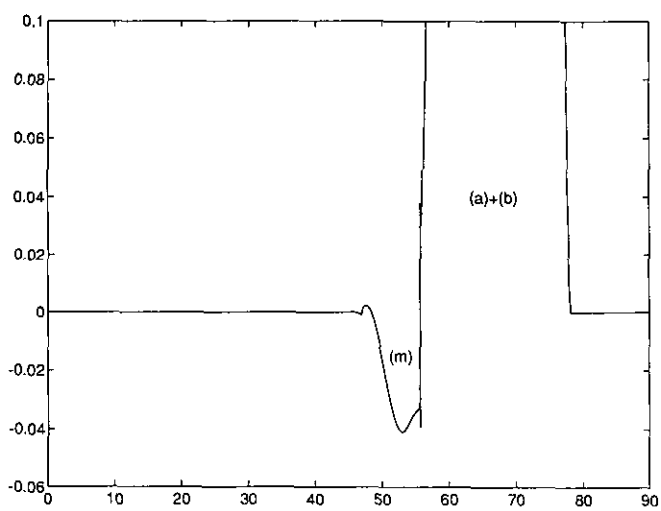

FIG. 2. Compacton interaction, $t = 10$.

TABLE III

Compacton Interaction

t	(a)	(b)	(c)	(m)	(n)
0	2.667	0.667	—	—	—
10	***	***	—	−0.041	—
20	2.667	0.659	—	−0.041	—
30	2.667	0.663	0.037	−0.041	—
40	2.667	0.664	0.037	−0.041	—
45	***	0.664	***	***	—
55	2.667	0.664	0.035	−0.042	—
65	***	***	0.035	−0.042	−0.041
75	2.667	0.656	0.035	−0.042	−0.041

Note. Amplitudes of the different waves as functions of time.

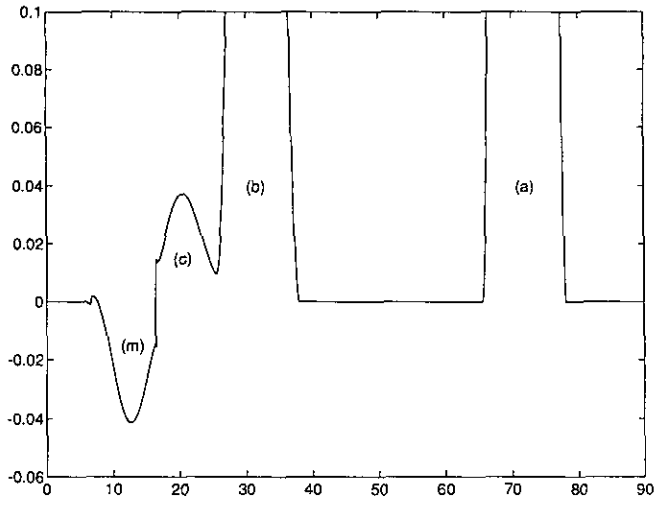

FIG. 4. Compacton interaction, $t = 30$.

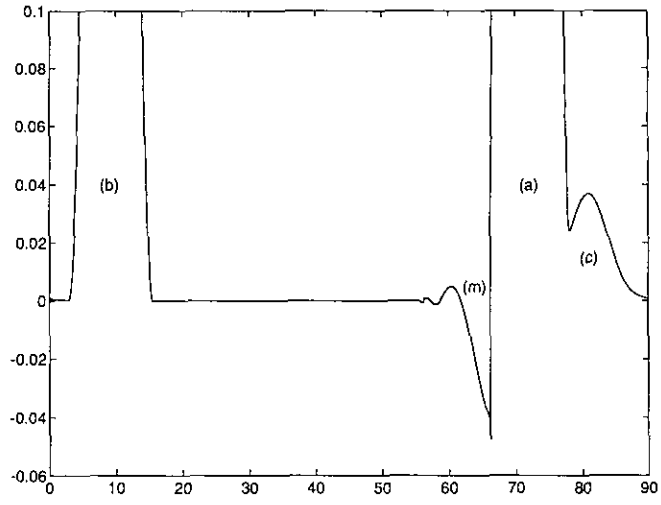

FIG. 6. Compacton interaction, $t = 45$.

2.674. At $t = 55$ (Fig. 7) both (m) and (c) have crossed through (a), and (b) is about to collide a second time with (a).

Figure 8 depicts the situation at $t = 65$ during the second collision of (a) and (b); a comparison with Fig. 2 is in order. A new negative wave (n) is being born as a consequence of this collision; its height and shape are the same as those of (m), born in the first (a)–(b) interaction. Figure 9 corresponds to the final time $t = 75$ and should be compared with Fig. 3.

We see in Table III that, when two compactons interact, the tallest emerges with its amplitude unchanged (or at least unchanged within the accuracy of the experiment). The short compacton, however, undergoes a decrease in amplitude. Compactons interact almost elastically and the equation reveals a strong tendency to oppose radiation; see, e.g., the long flat stretch in Fig. 5. Another feature worth noting is that (Fig. 9) whenever a negative wave is immediately to the *left* of a positive wave there is a shock between them. On the other hand, a negative wave immediately to the *right* of a positive wave does not lead to the formation of a shock.

APPENDIX

Here we consider the initial value problem for (1), subject to periodic boundary conditions. The case of the pure initial value problem may be treated similarly.

We multiply (1) by a test function χ and integrate by parts to arrive at

$$(u_T, \chi) - (u^2, \partial_x \chi) + (\partial_x u^2, \partial_x^2 \chi) = 0, \tag{A1}$$

where $(\cdot, \cdot)$ denotes the standard L^2 inner product. By a weak

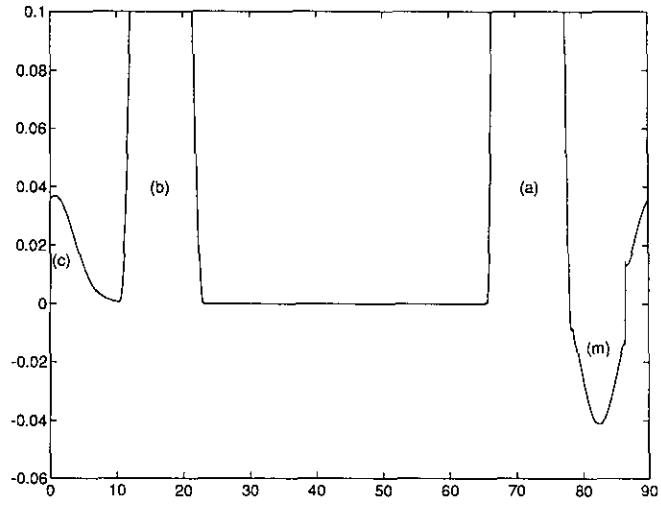

FIG. 5. Compacton interaction, $t = 40$.

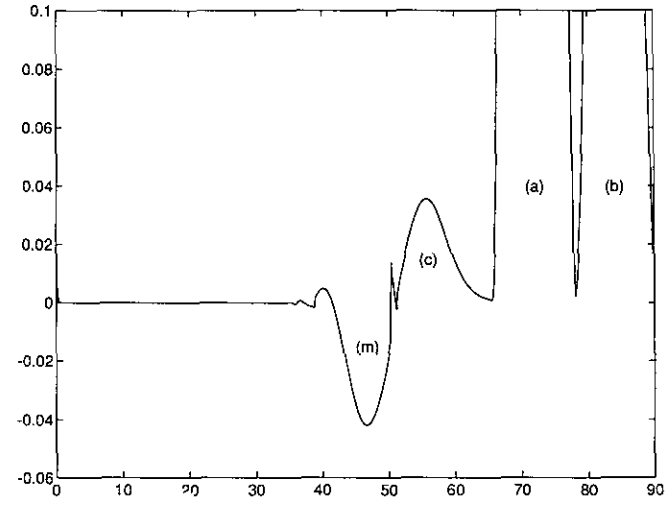

FIG. 7. Compacton interaction, $t = 55$.

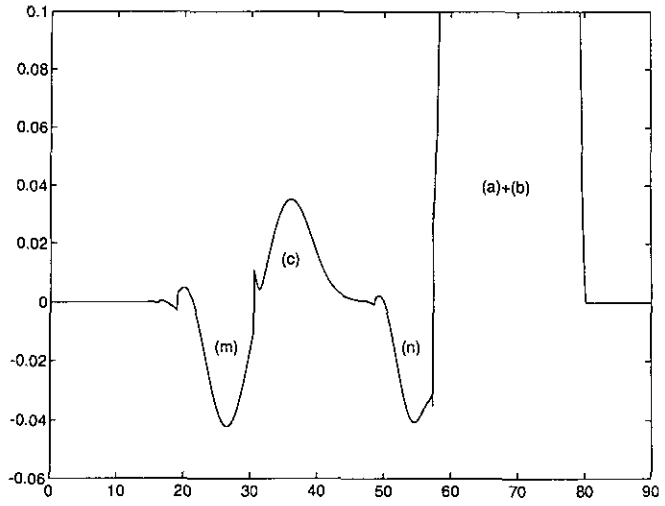

FIG. 8. Compacton interaction, $t = 65$.

solution of (1) we understand a mapping $u \in \mathcal{C}([0, T_{\max}], H^2) \cap \mathcal{C}^1([0, T_{\max}], L^2)$ such that (A1) holds for each time $0 \leq T \leq T_{\max}$ and each $\chi \in H^2$. Note that H^2 is closed under function multiplication and therefore, for a weak solution, u^2 is, at each time T, in H^2. Also H^2 is embedded in the space of continuous functions and thus weak solutions are continuous.

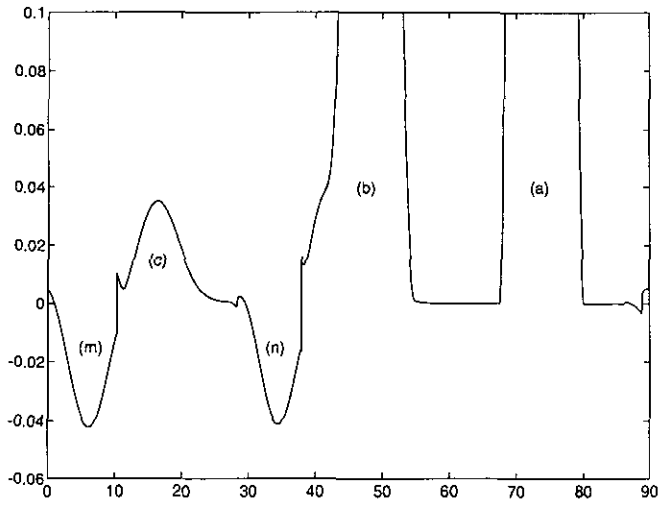

FIG. 9. Compacton interaction, $t = 75$.

The following result was obtained as a consequence of a conversation with Professor Ch. Elliott.

THEOREM 1. *A weak solution of* (1) *taking nonnegative values at time* 0 *remains nonnegative at all times* $0 \leq T \leq T_{\max}$.

Proof. If u_- denotes the negative part of u, then $(u_-)^2$ is, for each fixed time T, an H^2 function that can play the role of χ in (A1). This leads to the equality

$$(u_T, (u_-)^2) - (u^2, \partial_X(u_-)^2) + (\partial_X u^2, \partial_X^2(u_-)^2) = 0.$$

It is now possible to replace u_- by u; this does not change the value of the inner products because the second factor of each inner product vanishes at the values of X for which u_- and u are different. This yields

$$((u_-)_T, (u_-)^2) - ((u_-)^2, \partial_X(u_-)^2) + (\partial_X(u_-)^2, \partial_X^2(u_-)^2) = 0,$$

a formula that readily implies $((u_-)_T, (u_-)^2) = 0$ or, in other words,

$$\frac{d}{dt}\int (u_-)^3\, dX = 0.$$

If this integral vanishes at time 0, then it vanishes at all later times. ∎

The same result is true by changing "nonnegative" into "*nonpositive.*"

ACKNOWLEDGMENTS

This research has been supported by project DGICYT PB92-254.

REFERENCES

1. J. de Frutos and J. M. Sanz-Serna, *J. Comput. Phys.* **103,** 160 (1992).
2. J. de Frutos and J. M. Sanz-Serna, "Erring and Being Conservative," in *Numerical Analysis 1993,* edited by D. F. Griffiths and G. A. Watson (Longman, London, 1994), p. 75.
3. J. de Frutos and J. M. Sanz-Serna, Applied Mathematics and Computation Reports, Report 1994/4, Universidad de Valladolid.
4. Ph. Rosenau and J. M. Hyman, *Phys. Rev. Lett.* **70,** 564 (1993).
5. J. M. Sanz-Serna and I. Christie, *J. Comput. Phys.* **39,** 94 (1981).